

Potassium Currents in Precursor Cells Isolated From the Anterior Subventricular Zone of the Neonatal Rat Forebrain

R. R. STEWART,¹ T. ZIGOVA,² AND M. B. LUSKIN²

¹Laboratory of Molecular and Cellular Neurobiology, National Institute on Alcohol Abuse and Alcoholism, Bethesda, Maryland 20892-8115; and ²Department of Cell Biology, Emory University School of Medicine, Atlanta, Georgia 30322-3030

Stewart, R. R., T. Zigova, and M. B. Luskin. Potassium currents in precursor cells isolated from the anterior subventricular zone of the neonatal rat forebrain. *J. Neurophysiol.* 81: 95–102, 1999. The progenitor cells from the anterior part of the neonatal subventricular zone, the SVZa, are unusual in that, although they undergo division, they have a neuronal phenotype. To characterize the electrophysiological properties of the SVZa precursor cells, recordings were made of potassium and sodium currents from SVZa cells that were removed from postnatal day 0–1 rats and cultured for 1 day. The properties of the delayed rectifier and A-type potassium currents were described by classical Hodgkin and Huxley analyses of activation and inactivation. In addition, cells were assessed under current clamp for their ability to generate action potentials. The A-type potassium current ($I_{K(A)}$) was completely inactivated at a holding potential of -50 mV. The remaining potassium current resembled the delayed rectifier current ($I_{K(DR)}$) in that it was blocked by tetraethylammonium (TEA; IC_{50} 4.1 mM) and activated and inactivated slowly compared with $I_{K(A)}$. The conductance-voltage (G - V) curve revealed that G increased continuously from 0.2 nS at -40 mV to a peak of 2.6 nS at $+10$ or $+20$ mV, and then decreased for voltages above $+30$ mV. Activation time constants were largest at -40 mV (~ 11 ms) and smallest at 100 mV (~ 1.5 ms). The properties of $I_{K(A)}$ were studied in the presence of 20 mM TEA, to block $I_{K(DR)}$, and from a holding potential of -15 mV, to inactivate both $I_{K(DR)}$ and $I_{K(A)}$. $I_{K(A)}$ was then allowed to recover from inactivation to negative potentials during 200- to 800-ms pulses. Recovery from inactivation was fastest at -130 mV (~ 21 ms) and slowest at -90 mV (~ 135 ms). Inactivation was voltage independent from -60 to $+60$ mV with a time constant of ~ 15 ms. At steady state, $I_{K(A)}$ was half inactivated at -90 mV. $G_{K(A)}$ increased from 0.2 nS at -60 mV to a peak of 2.4 nS at $+40$ mV. Finally, the activation time constants ranged from ~ 1.9 ms at -50 mV to 0.7 ms at $+60$ mV. The properties of $I_{K(A)}$ resembled those of $I_{K(A)}$ found in differentiating cerebellar granule neurons. Most SVZa cells had sodium currents (28/32 cells). However, in current clamp 11 of 12 cells were incapable of generating action potentials from voltages of -30 to -100 mV, suggesting that the available current densities were too low to support excitability.

INTRODUCTION

In the olfactory system of mammals new neurons are generated well into adulthood from two separate populations of precursor cells. One group originates from the olfactory epithelium and the other from the anterior region of the

subventricular zone (SVZa) of the forebrain (Luskin 1993; Magrassi and Graziadei 1995). Of particular interest are the precursor cells of the SVZa, whose progeny migrate long distances from the SVZa to the olfactory bulb, where they differentiate into two types of interneurons: granule and periglomerular cells (Jankovski and Sotelo 1996; Luskin 1993; Zigova et al. 1996). SVZa precursor cells are unusual in that they exhibit neuronal characteristics as evidenced by labeling with TuJ1, an antibody against neuron-specific class III β -tubulin. In addition, unlike other immature neurons, they migrate tangentially without the aid of radial glial cells and continue dividing as they migrate to the olfactory bulb (Luskin 1993; Menezes and Luskin 1994; Zigova et al. 1996). The migration of SVZa-derived cells has been found to require the expression of the relatively nonadhesive, polysialated form of neural cell adhesion molecule (Hu et al. 1996; Ono et al. 1994; Tomasiewicz et al. 1993). Morphologically, the cells traversing the pathway have the features of migrating neurons. They consist of a cell body that is ~ 8 - μ m wide by 12- to 15- μ m long, a thick caliber leading process with a growth cone, and a thin caliber trailing process (Jankovski and Sotelo 1996; Luskin 1993; Luskin and Boone 1994; Menezes and Luskin 1994; Zigova et al. 1996). Thus, except for their ability to divide, SVZa-derived cells have features associated with postmitotic neurons.

Many of the described properties of SVZa precursor cells in vivo are present in vitro. Thus precursor cells in culture for 1–8 days continue to express the neuron-specific marker class III β -tubulin, and to divide (Luskin et al. 1997; Zigova et al. 1996). Because nothing is known about the electrophysiological properties of the SVZa precursor cells, we wanted to know if they resemble immature neurons. Therefore we have undertaken a survey of their electrical characteristics with descriptions and kinetic analyses of the types of potassium currents recorded with the use of the whole cell patch clamp. The types of potassium currents present in these cells after 1 day in vitro include A-type and tetraethylammonium (TEA)-sensitive, delayed rectifier and calcium-activated outward potassium currents, which are also found in other types of neurons, such as cerebellar granule cells (Cull-Candy et al. 1989; Fagni et al. 1991; Hockberger et al. 1987; Stewart et al. 1995).

METHODS

Culturing SVZa neuronal precursor cells

The SVZa was removed from postnatal day (P) P0–P1 rat pups with our established National Institutes of Health approved proce-

The costs of publication of this article were defrayed in part by the payment of page charges. The article must therefore be hereby marked "advertisement" in accordance with 18 U.S.C. Section 1734 solely to indicate this fact.

dures (Luskin et al. 1997; Zigova et al. 1996), placed in 100 mM sucrose in dissecting solution (Hank's Balanced Salt Solution, Life Technologies, Gaithersburg, MD) with 1 mM sodium pyruvate and 10 mM *N*-2-hydroxyethylpiperazine-*N'*-2-ethanesulfonic acid (HEPES), pH 7.4, and dissociated mechanically. For some experiments, cerebellar granule cells from P5 rat pups were used. Cells were plated on poly-DL-ornithine-coated (Sigma-Aldrich Fine Chemicals, St. Louis, MO) 35-mm culture dishes and maintained for 1 day in vitro (DIV) in medium consisting of Minimal Essential Medium (MEM, Life Technologies), 1% B27 supplement (Life Technologies), α -D-glucose, sodium pyruvate, and 10% horse serum (HyClone Laboratories, Logan, UT).

To verify that SVZa precursor cells were being selected for recording, cultured cells were fixed for 30 min in 4% paraformaldehyde/0.1 M phosphate buffered saline (PBS), rinsed twice in PBS, and then placed in blocking buffer for 30 min before labeling with a monoclonal antibody against class III β -tubulin (Sigma-Aldrich) as described previously (Lee et al. 1990; Luskin et al. 1997). The morphologies of the class III β -tubulin positive cells and of the recorded cells were then compared.

Whole cell patch-clamp recordings

Patch electrodes of 4–8 M Ω were made from hard borosilicate glass (World Precision Instruments, Sarasota, FL) on a Brown-Flaming electrode puller (Sutter Instrument, Novato, CA). Electrodes were coated with Sylgard (Corning, Corning, NY) as described in Hamill et al. (1981). The internal pipette solution contained (in mM) 142 KCl, 10 NaCl, 2 MgCl₂, 11 ethylene glycol-bis(β -aminoethyl ether)-*N,N,N',N'*-tetraacetic acid (EGTA), and 10 HEPES (pH was adjusted to 7.2 with KOH); the external solution contained (also in mM) 150 NaCl, 5 KCl, 1 CaCl₂, 10 glucose, 0.0003 tetrodotoxin (TTX, Sigma-Aldrich), and 10 HEPES (pH was adjusted to 7.4 with NaOH). In some experiments, the TTX was omitted. The signal from the patch head stage was connected to an EPC7 patch-clamp amplifier (Medical Systems, Greenvale, NY) and was filtered at 2 and 10 KHz (–3 db, 8-pole Bessel filter, Model 902, Frequency Devices, Haverhill, MA). Data were digitized with an A/D converter (Digidata 1200, Axon Instruments, Foster City, CA), stored on an IBM-based computer, and acquired using pClamp 6.0 programs (Axon Instruments). Records were analyzed with Clampfit 6 (Axon Instruments). Graphs and final curve fits were made by using SigmaPlot version 2.01 (SPSS, Chicago, IL). Results are expressed as means \pm SE, unless indicated otherwise. *N* represents the number of cells.

RESULTS

General characteristics of SVZa precursor cells

Figure 1, *A–D*, shows examples of SVZa cells from which recordings were made. Each cell had a thick process (large arrows) and a cell body length of 10–12 μ m. In Fig. 1*C*, the cell was bipolar and had a short thick process from which a thinner caliber process extended (small arrow). SVZa precursor cells in situ and in vitro express the neuron-specific protein class III β -tubulin, which is recognized by the monoclonal antibody TuJ1 (Lee et al. 1990; Luskin et al. 1997; Menezes and Luskin 1994; Zigova et al. 1996). Figure 1, *E–G* shows SVZa cells labeled by anticlass III β -tubulin. The morphologies of the recorded and the antibody-labeled cells were similar in cell body size and process thickness and length.

The mean resting membrane potential of the recorded cells was -31.8 ± 9.6 (mean \pm SD, *n* = 122). Although a majority of SVZa cells had sodium currents (28/32 cells

tested), most (11/12) were unable to generate overshooting action potentials when held in current clamp at -30 to -100 mV and depolarized with current steps of 40-ms duration. An example is in Fig. 2.

Delayed rectifier potassium current ($I_{K(DR)}$)

$I_{K(DR)}$ was measured in individual SVZa precursor cells by stepping the voltage from a holding potential of -60 mV to -50 mV up to $+100$ mV in 10-mV increments (Fig. 3*A*). At a holding potential of -60 mV, all of A-type potassium current ($I_{K(A)}$) was inactivated. In the Hodgkin–Huxley model, $I_{K(DR)}$ is represented by the equations $I_K = G_K(V - E_K)$ and $G_K = n^4 \bar{G}_K$, where G_K is conductance in pA/mV (nS), *n* represents the activation parameter, \bar{G}_K is the maximal conductance, *V* is the membrane potential, and E_K is the potassium reversal potential. In Fig. 3*B*, the peak current and peak current density-voltage relations are plotted. From the peak current values, the steady-state conductance-voltage (G_K -*V*) relation was determined assuming E_K to be -83 mV (Fig. 4*A*). Thus the conductance increased continuously from 0.2 ± 0.02 nS at -40 mV to a peak conductance (\bar{G}_K) of 2.6 ± 0.3 nS at $+20$ mV and then decreased for voltages above $+30$ mV to a value of 1.4 ± 0.2 nS at 100 mV. In Fig. 4*B*, the steady-state activation (n_∞) curve was generated by calculating each value of *n* using the equation $n(V) = [G_K(V)/\bar{G}_K]^{1/4}$. Next, the points up to the peak conductance were fitted with the Boltzmann equation $n(V) = \{1 + \exp[(V - V_n)/k_n]\}^{-1}$, where the voltage at half-maximal amplitude (V_n) was -50 mV and the slope factor (k_n) was 15 mV.

To determine the time dependence of *n*, activation time constants were estimated assuming that $n(t)^4 = A[1 - \exp(-t/\tau_n)]^4 + C$, where *A* is the peak current amplitude and *C* is the offset. The time constants were largest at -40 mV (~ 11 ms) and smallest at 100 mV (~ 1.5 ms, Fig. 4*C*). The time constant versus voltage curve could be approximated with the continuous function $\tau_n(V) = 0.27 \cdot \exp\{-[(V - 38.35)/22.07]\} + 1.65$. As expected, the activation process was time- and voltage-dependent.

As shown in Fig. 5*A*, $I_{K(DR)}$ was inactivated during long depolarizing voltage steps. The inactivation time constants were measured from currents flowing during voltage steps of ~ 8 s duration to -30 , -15 , 0 , 15 , and 30 mV from a holding potential of -60 mV (Fig. 5*A*). One and sometimes two inactivation time constants could be fitted to each current trace. The faster of the two time constants was estimated assuming a single exponential and a sloping baseline that approximated the slower of the two time constants; the fast inactivating time constants are plotted versus voltage in Fig. 5*B*. $I_{K(DR)}$ inactivated with time constants of $1,145 \pm 193$ ms (*n* = 8) at -30 mV and 619 ± 63 ms (*n* = 11) at $+30$ mV. The slow time constant was estimated to be ~ 5.7 s at -30 mV, ~ 2.6 s at 0 mV, and ~ 5.1 s at $+30$ mV. The ability of $I_{K(DR)}$ to recover from inactivation was determined by holding the membrane potential at -15 mV to inactivate all K currents, stepping the voltage to -70 or -60 mV for durations ranging from 0 to ~ 8 s to allow recovery and then stepping the voltage to $+15$ mV for 480 ms (Fig. 6*A*). Figure 6*B* shows an example of the time course for recovery of $I_{K(DR)}$. The continuous line represents the result of fitting the points with a rising exponential function. The recovery

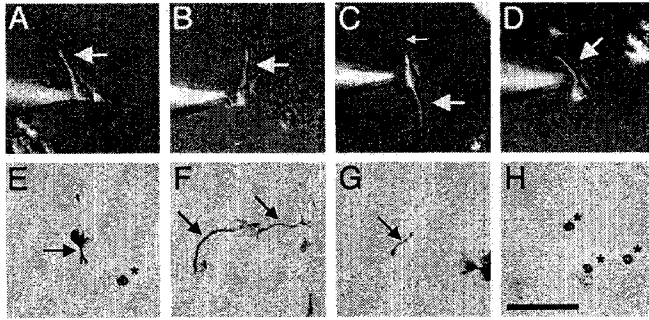


FIG. 1. Morphology and identification of SVZa, the anterior part of the neonatal subventricular zone, precursor cells after 1 day in vitro. A-D: examples of cells from which recordings were made. Each cell has a thick process (large arrows in A-D) ~20-30 μm in length. C: thin process (small arrow) projects opposite to thick process. E-G: SVZa cells stained by an antibody to class III β -tubulin (TuJ1). Cell stained in E is morphologically similar to SVZa cells in A, B, and D. H: negative control in which the primary antibody was omitted. Cells indicated by the asterisks in panels E and H are nonspecifically stained red blood cells. Scale bar in panel H represents 50 μm and also applies to panels A-G.

time constants were 1.78 ± 0.25 s ($n = 5$) at -70 mV and 3.38 ± 0.95 s ($n = 3$) at -60 mV.

To measure steady-state inactivation of $I_{K(DR)}$, voltage pulses to $+50$ mV were given from various holding potentials. However, before each test pulse, the leak currents at each holding potential were collected using four hyperpolarizing pulses ($|$ holding potential + depolarizing potential $|/4$ or P/4 subtraction), the voltage held for an additional 15 s at -70 mV up to -10 mV in 10-mV increments, and the leak compensated for during the acquisition (Fig. 7A). In Figure 7B, the peak $I_{K(DR)}$ is plotted as a function of holding potential and the data points fitted with the Boltzmann equation. The half-maximal inactivation for the curve in Fig. 7B was -47.4 mV with a slope factor of 5.1 mV. The mean half-maximal steady-state inactivation as determined from fitting the individual curves occurred at -50.1 ± 2.2 mV ($n = 6$).

TEA is known to block a subset of potassium currents in many types of neurons (Dolly and Parcej 1996; Grissmer et al. 1994; Hockberger et al. 1987; Rudy 1988). An example of the slowly inactivating I_K exposed to 1 mM TEA during voltage steps to 0 mV is shown in Fig. 8A. The IC_{50} for TEA on the outward current was 4.1 mM ($n = 5-13$, Fig.

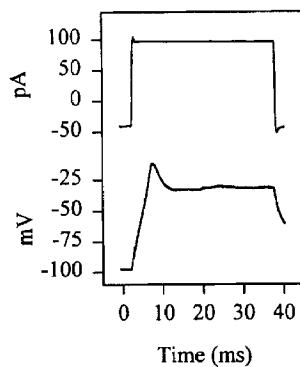


FIG. 2. Membrane potential response of a cultured SVZa progenitor cell to current step in current clamp. Top: depolarizing current step. Bottom: membrane potential during current step. Membrane potential did not reach 0 mV. I_{Na} was detectable in this cell under voltage clamp (not shown).

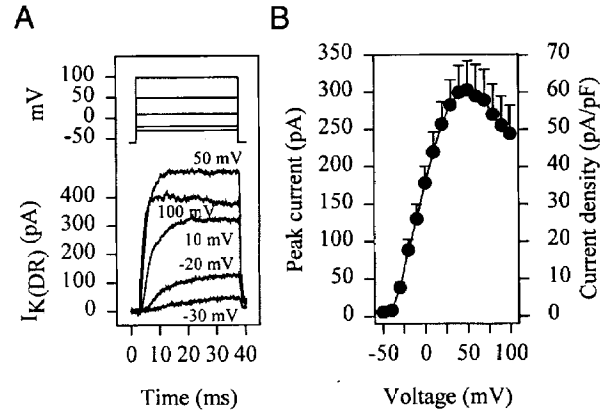


FIG. 3. Delayed rectifier potassium currents ($I_{K(DR)}$) in cultured SVZa cells. A, top: voltage steps from -60 to $+100$ mV from a holding potential of -60 mV. Current traces were leak subtracted (P/4). Current evoked at 100 mV is smaller and inactivates compared with the current elicited at $+50$ mV. B: current- and current density-voltage relations. Current activates at approximately -40 mV, reaches a peak at $+50$ mV, and then decreases for voltage steps from $+60$ to $+100$ mV. Data points are connected by straight lines. These properties are typical of delayed rectifier potassium currents.

8B) and was estimated by fitting with the logistic equation $y = (y_{max} - y_{min})/[1 + (x/IC_{50})^z] + y_{min}$, where x is the concentration of applied TEA, IC_{50} is the concentration of TEA at half-maximal inhibition, z is the Hill coefficient or slope, y_{max} is the maximum amplitude, and y_{min} is the minimum amplitude.

The presence of $I_{K(Ca)}$ was tested by blocking calcium entry with 100 μM CdCl_2 (Fig. 9). Indeed, in seven of nine cells, the peak currents evoked during voltage steps to 0 mV from a holding potential of -70 mV were greater in an external solution with 1 mM CaCl_2 than in solution with 100 μM CdCl_2 substituted for the 1 mM CaCl_2 . The mean current density for these cells was 25.7 ± 6.4 pA/

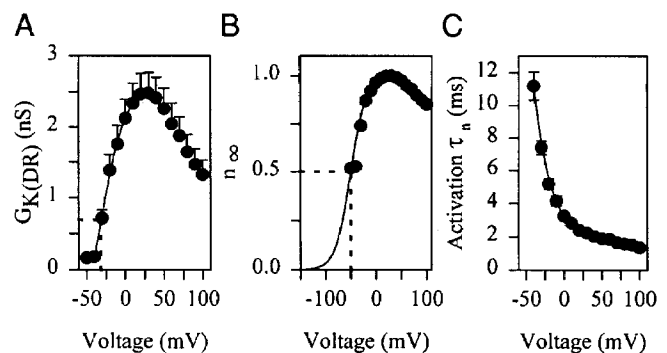


FIG. 4. Activation properties of $I_{K(DR)}$ in cultured SVZa cells. A: conductance-voltage curve was determined assuming E_K to be -83 mV. Conductance reached peak at $+10$ to $+20$ mV and decreased continuously from $+30$ to $+100$ mV. Data were fitted using the Boltzmann equation $y = [(A - C)/(1 + \exp[(V - V_{1/2})/k])] + C$ with the voltage (V) restricted from -40 to $+20$ mV (—). Voltage at half activation ($V_{1/2}$) was -31.4 mV, A was 2.6, C was -1.3 , and k was -16.4 mV. B: steady-state activation parameter n (n_{∞}) vs. voltage curve. n_{∞} curve was fitted with the Boltzmann equation (—). - - -, each gating particle was half activated at -50 mV; slope factor was -15 mV. C: activation time constant as a function of voltage. —, curve fit using the continuous function $\tau_n(V) = 0.27 \cdot \exp\{-[(V - 38.35)/22.07]\} + 1.65$ described in RESULTS.

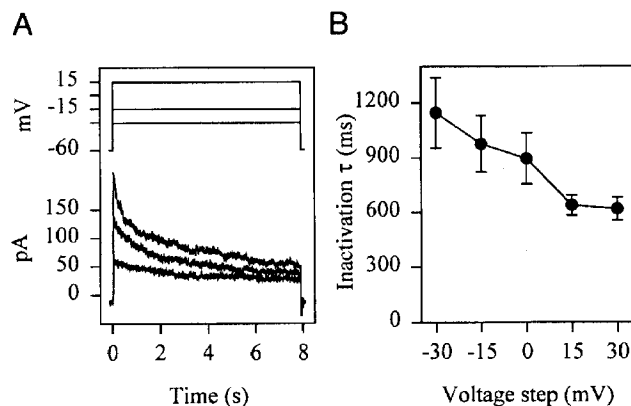


FIG. 5. Time-dependent inactivation of $I_{K(DR)}$ in cultured SVZa cells. *A*: holding potential of -60 mV was maintained for 30 s before stepping to voltages from -30 to $+30$ mV in 15-mV increments. *B*: faster of 2 time constants is plotted vs. membrane potential. Data points are connected by straight lines. Inactivation was voltage-dependent, occurring more rapidly during larger depolarizations.

pF in $100 \mu\text{M CdCl}_2$ and increased by 6.6 ± 2.0 pA/pF in 1 mM CaCl_2 . In two cells, the current density decreased by 1.3 and 3.1 pA/pF. At 40 mV, the current density in the presence of 1 mM CaCl_2 was decreased in five cells (range 2.5–23.2 pA/pF) and increased in four of nine cells (range 0.8–6.0 pA/pF). These results indicate that for voltage steps to 0 mV, which is near the peak of calcium current I - V curves (Bardoni and Belluzzi 1993; Bardoni et al. 1996; Stewart et al. 1995), a 26% increase in outward current occurred in 78% of the cells. Thus most SVZa precursor cells exhibit outward current carried by $I_{K(Ca)}$.

A-type potassium current ($I_{K(A)}$)

The outward current that remained in the presence of 20 or 100 mM TEA exhibited the properties of $I_{K(A)}$; it activated and inactivated rapidly (Fig. 10A) and was half-inactivated

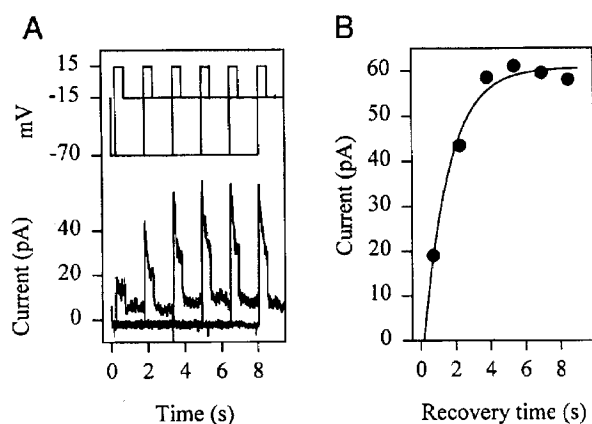


FIG. 6. Recovery from inactivation of $I_{K(DR)}$ by cultured SVZa cells. *A*, top: holding potential was -15 mV. Voltage steps to $+15$ mV were made from a prepulse potential of -70 mV of variable duration. Bottom: currents evoked during voltage steps to $+15$ mV exhibited inactivation. A persistent outward current was evident at -15 mV. *B*: peak outward current vs. recovery time is plotted for each prepulse voltage from -70 to -40 mV. The curve was fitted using a single rising exponential function (solid line).

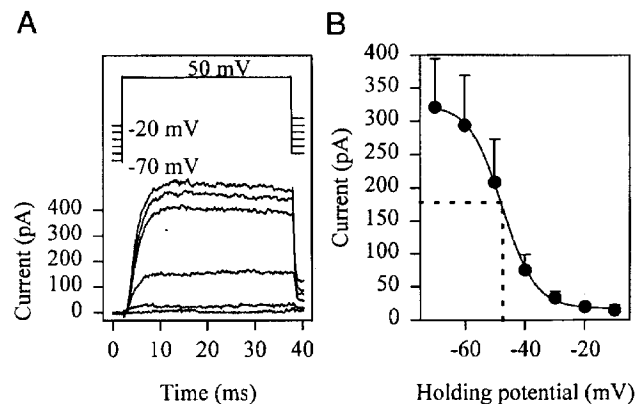


FIG. 7. Steady-state inactivation of $I_{K(DR)}$ in cultured SVZa cells. *A*, top: voltage step to 50 mV from various holding potentials. Bottom: currents evoked by voltage steps to 50 mV after holding the membrane potential for 30 s at each indicated voltage. Largest outward current was evoked by holding at -70 mV and the smallest was evoked after holding at -10 mV. Records were leak subtracted using 4 voltage pulses each $1/4$ amplitude of the depolarizing voltage step ($P/4$). *B*: peak current vs. holding voltage. —, fitted Boltzmann curve with $A = 362.1$, $C = 19.5$, $k = 5.1$, and $V_{1/2} = -47.4$ mV. Mean voltage at half-maximal inactivation ($V_{1/2}$) for the 6 individual curves was -50.1 ± 2.2 mV.

at a holding potential of -90 mV. The Hodgkin–Huxley model for an inactivating sodium current was used to characterize $I_{K(A)}$ (Bardoni and Belluzzi 1993; Hodgkin and Huxley 1952). The equations used to describe $I_{K(A)}$ were $I_{K(A)} = G_{K(A)}(V - E_K)$ and $G_{K(A)} = a^3 \bar{G}_{K(A)} h_a$, where $\bar{G}_{K(A)}$ is the maximal conductance, a is the activation parameter, h_a is the inactivation parameter, E_K is -83 mV, and V is the membrane voltage. To determine the current-voltage relation, the current traces were analyzed first for inactivation using an exponential decay function. Next, the current was extrapolated back to $t = 0$, and these values minus the plateau or offset currents were used in the current-voltage relation. The time dependence of inactivation for various voltage steps is shown in Fig. 10B. τ_{ha} was voltage-independent,

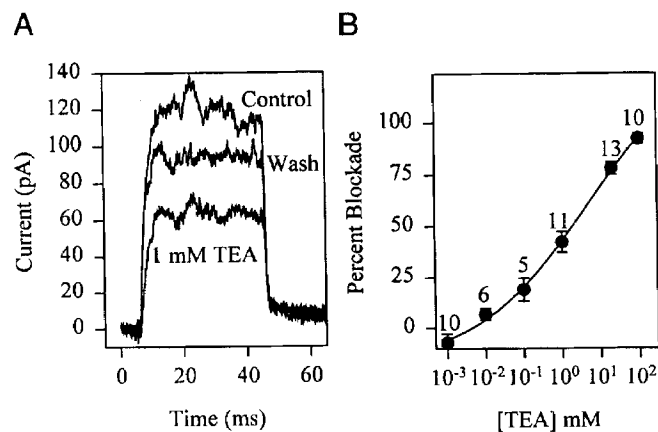


FIG. 8. Sensitivity of $I_{K(DR)}$ to tetraethylammonium (TEA) in cultured SVZa cells. *A*: control current, current during block by 1 mM TEA , and current after washing for 30 s. *B*: concentration-percent inhibition curve for TEA. Data were fitted with the logistic equation and the IC_{50} for TEA was 4.1 mM , which indicates K channels with intermediate sensitivity. Value of z , the slope factor, was 0.3. The number above each data point indicates number of cells at each concentration.

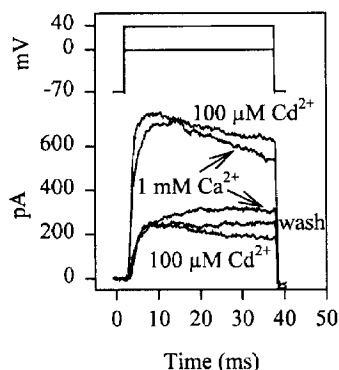


FIG. 9. Calcium-activated potassium current in cultured SVZa cells as determined by sensitivity to 100 μM CdCl_2 . Voltage was held at -70 mV and stepped to 0 and $+40$ mV (top 2 voltage traces). Current records obtained at $+40$ mV (top 2 current traces) and at 0 mV (bottom 3 current traces). For both voltage steps, currents were measured in 100 μM CdCl_2 , in 1 mM CaCl_2 , and after returning to 100 μM CdCl_2 (Wash). Capacitance of this cell was 5.5 pF and at 0 mV the increase in current density in 1 mM CaCl_2 was 12.4 pA/pF. Most SVZa cells (7/9) had detectable $I_{K(\text{Ca})}$ that contributed to $I_{K(\text{DR})}$.

having a mean value of ~ 15 ms for all voltages tested. Inactivation at steady state (SSI) is shown in Fig. 11. The voltage was held at -15 mV, hyperpolarized to -20 down to -130 mV in 10 mV increments, and stepped to the test voltage of $+20$ mV for 100 ms. The voltage at half-peak amplitude ($V_{1/2}$) was -90.4 ± 1.5 mV ($n = 23$, Fig. 11). Fitting the SSI curve in Fig. 11B with the Boltzmann equation revealed a peak of 174 pA, an offset of 18.8 pA, a $V_{1/2}$ of -89.9 mV, and a slope of 6.83. From a holding potential of -15 mV, $I_{K(A)}$ recovered (Fig. 12A) with a time constant that was voltage dependent (Fig. 12, B and C). Recovery was fastest at -130 mV with a time constant of ~ 21 ms ($n = 26$) and slowest at -90 mV (the $V_{1/2}$ of steady-state inactivation) with a peak of ~ 135 ms ($n = 12$). The curve in Fig. 12C was generated using the equation $\tau_{\text{ha}} =$

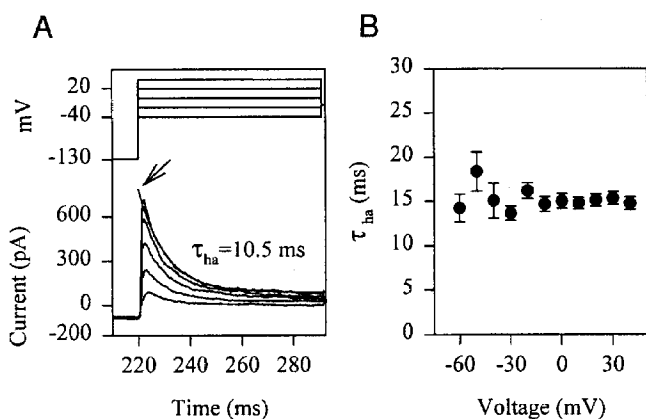


FIG. 10. Characteristics of $I_{K(A)}$ in cultured SVZa cells in the presence of 20 or 100 mM TEA to block $I_{K(\text{DR})}$. A, top: voltage was held at -15 mV, hyperpolarized to -130 mV for 220 ms, and then stepped for 80 ms to -60 mV up to $+40$ mV in 10 mV increments. Bottom: voltage steps to -40 mV (smallest) up to $+30$ mV (largest). Arrow points to solid line, which represents the single exponential curve fit to the falling phase of the current. Inactivation time constant (τ_{ha}) was 10.5 ms. B: inactivation time constants at each activation voltage. Time constants were voltage independent and ~ 15 ms.

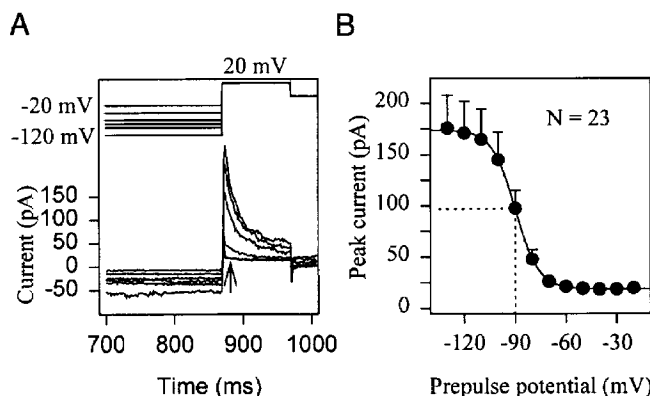


FIG. 11. Steady-state inactivation of $I_{K(A)}$ in cultured SVZa cells. A, top: voltage step to 20 mV from various prepulse hyperpolarizing potentials. Holding voltage was -15 mV. Bottom: currents evoked by voltage steps to 20 mV after holding the membrane potential for 850 ms at each voltage indicated at the top of A. Largest outward current was evoked by holding at -130 mV, and the smallest was evoked after holding at -10 mV. Arrow points to where current measurements were made. B: current measured at the arrow in A vs. holding voltage. Fitting the steady-state inactivation curve with the Boltzmann equation resulted in $A = 174$ mV, $C = 18.8$ mV, $k = 6.83$ mV, and $V_{1/2} = -89.9$ mV. Solid line, results of the fit. Mean voltage at half-maximal inactivation ($V_{1/2}$) for the 23 individual curves was -90.4 ± 1.5 mV.

$14.475 + (0.0146 \cdot V) + 1/[9230.29 \cdot \exp(V \cdot 0.1688) + 2.9351 \cdot 10^{-5} \cdot \exp(-V \cdot 0.0589)]$ and includes inactivation time constants from Fig. 10B. Thus for any hyperpolarizing voltage step, there is an interplay between inactivation and recovery from inactivation that is exhibited in the bell-shaped behavior of the recovery time constant.

Plotting the extrapolated peak $I_{K(A)}$ as a function of voltage showed that threshold for activation was approximately -50 mV (Fig. 13A). The conductance-voltage relation was determined by calculating $G_{K(A)}$ from $I_{K(A)}/(V - E_K)$ with $I_{K(A)}$ equal to the extrapolated current at each voltage step

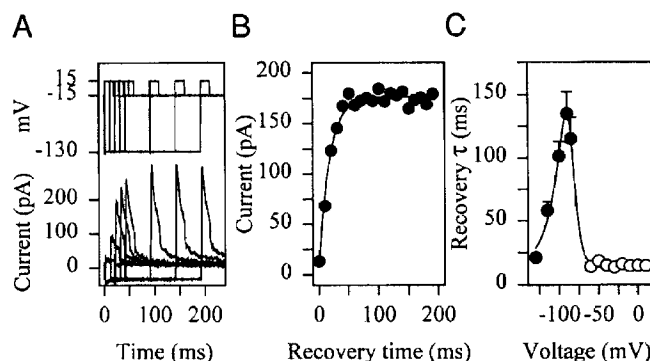


FIG. 12. Recovery of $I_{K(A)}$ in cultured SVZa cells from inactivation at different holding potentials. A: recovery traces at -130 mV. Top: voltage protocol with prepulse holding potential to -130 mV of variable duration. Test voltage step was to $+15$ mV. B: peak current vs. recovery time at -130 mV. —, fitted data assuming a rising exponential equation. Time constant was 17.7 ms. C: recovery time constant vs. recovery potential (\bullet). Means were fitted using the equation $y = q + (bcV) + 1/[c \cdot \exp(V \cdot d) + f \cdot \exp(-V \cdot j)]$. Fit values were $q = 14.48$, $b = 0.0146$, $c = 9320.3$, $d = 0.169$, $f = 2.93 \times 10^{-5}$, and $j = 0.0589$. \circ , mean inactivation time constants from Fig. 10B. Thus bell-shaped curve illustrates voltage dependence of exponential time constant of appearance or recovery from inactivation.

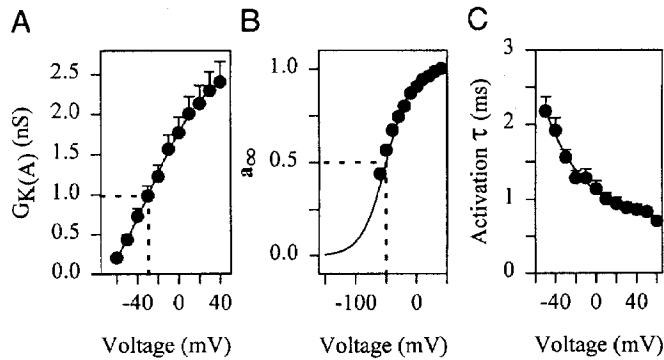


FIG. 13. Activation properties of $I_{K(A)}$ in cultured SVZa cells. **A**: conductance ($G_{K(A)}$) vs. voltage curve. —, result of fitting data with the Boltzmann equation $G_a(V) = A/[1 + \exp[(V - V_{1/2})/k]] + C$. Voltage at half-maximal conductance was -31.8 mV ($A = 2.8$ mV, $C = -0.7$ mV, $k = 30.2$ mV). **B**: activation at steady state (a_∞) vs. voltage curve calculated with the function $a_\infty(V) = [G_a(V)/\bar{G}_{K(A)}]^{1/3}$ where G_a is conductance as a function of voltage and $\bar{G}_{K(A)}$ is the maximal conductance. After fitting $a_\infty(V)$ with the Boltzmann equation as shown by solid line, voltage at half-maximal a_∞ was -50.0 mV and k was 20.0 mV. **C**: activation time constant (τ_a) as a function of voltage. Solid line, best fit to the data; described by the function $\tau_a(V) = 0.24 \cdot \exp\{-[(V - 22.80)/39.68]\} + 0.68$.

and E_K and V as described above. Using the Boltzmann equation $G_a(V) = A/[1 + \exp[(V - V_{1/2})/k]] + C$ to fit the G - V curve (Fig. 13A) produced slope factor k of 30.2 mV, $V_{1/2}$ of -31.8 mV, and A and C of 2.8 and -0.7 , respectively. The a_∞ or steady-state activation curve was calculated using $a_\infty(V) = [G_a(V)/\bar{G}_{K(A)}]^{1/3}$ as shown in Fig. 13B. Thus after fitting the curve with the Boltzmann equation, the activation parameter a was half-maximal at -50 mV and had a slope factor k of 20 mV. Activation time constants were determined for voltages from -50 to $+60$ mV in 10 -mV increments by fitting with the equation $a^3 h_a = \{A[1 - \exp(-t/\tau_a)]^3 + C\} + A \exp(-t/\tau_{ha})$, where A is the maximal current amplitude, τ_a is the activation time constant, τ_{ha} is the inactivation time constant, t is time, and C is the offset. These results are plotted as a function of voltage in Fig. 13C. The mean τ_a at -50 mV was 2.2 ± 0.2 ms ($n = 7$) and decreased to 0.7 ± 0.2 ms ($n = 7$) at $+60$ mV. These values are described by the function $\tau_a(V) = 0.24 \cdot \exp\{-[(V - 22.80)/39.68]\} + 0.68$.

There are several different types of α subunits (Kv1.4, Kv3.3–3.4, Kv4.1–4.3) that code for K channels with characteristics of $I_{K(A)}$ (Baldwin et al. 1991; Pak et al. 1991; Schröter et al. 1991; Serôdio et al. 1996; Stühmer et al. 1989; Vega-Saenz de Miera et al. 1992). However, Kv3.3 and Kv3.4 cannot be considered here because both are sensitive to external TEA ($IC_{50} < 1$ mM). To determine if the $I_{K(A)}$ reported here was produced by Kv1.4, which is blocked completely in external solution without potassium, we tested the effect of 0 K external solution on $I_{K(A)}$ (Pardo et al. 1992). Other types of potassium currents are reduced by 50 – 60% in this solution (Pardo et al. 1992). With $I_{K(DR)}$ blocked by 20 mM TEA, $I_{K(A)}$ was subjected to external solution with and without 5 mM potassium. In six cells, $I_{K(A)}$ was reduced by $51 \pm 3\%$. In addition, cerebellar neurons, which do not express Kv1.4, were cultured under similar conditions and $I_{K(A)}$ exposed to ± 5 mM potassium-containing medium. $I_{K(A)}$ was reduced by $40 \pm 14\%$ ($n = 5$).

Thus Kv1.4 does not appear to contribute significantly to the $I_{K(A)}$ recorded in SVZa precursor cells.

The sensitivity of $I_{K(A)}$ to 2 mM 4-aminopyridine (4-AP) was tested in external solutions containing 20 mM TEA to block $I_{K(DR)}$ and $I_{K(Ca)}$. In nine cells, $I_{K(A)}$ was reduced by $28 \pm 3\%$. The IC_{50} for 4-AP on most α subunits is ≤ 1.5 mM and Kv 1.4 and Kv 4.1–4.3 are fairly insensitive to 4-AP (Dolly and Parcej 1996; Serôdio et al. 1994, 1996). Because the $I_{K(A)}$ reported here does not have the properties of Kv 1.4, it is likely that members of the Kv4 series of subunits contribute to the generation of the $I_{K(A)}$. Both Kv4.2 and Kv4.3 mRNAs are expressed strongly in the CNS and in periglomerular and granule neurons of the olfactory bulb (Serôdio and Rudy 1998). In comparison, Kv4.1 mRNA has a limited distribution and is weakly expressed in the brain (Pak et al. 1991; Serôdio and Rudy 1998). The weak expression of Kv4.1 mRNA in granule neurons of adult olfactory bulb (Serôdio and Rudy 1998) suggests that the Kv4.1 subunit may also play a role in SVZa precursor cells.

DISCUSSION

We have characterized the properties of precursor cells isolated from the SVZa of P0–P1 rats and cultured for 1 day. The cultured SVZa precursor cells expressed neuron-specific tubulin and had morphological characteristics of neurons *in vivo* and *in vitro* as described previously (Luskin 1993; Luskin et al. 1997; Zigova et al. 1996). Moreover, SVZa precursor cells had resting potentials of approximately -32 mV and TTX-sensitive sodium currents, but were unable to generate action potentials from membrane potentials of -30 to -100 mV. Two general types of potassium currents, $I_{K(A)}$ and $I_{K(DR)}$, were described by their activation and inactivation characteristics and by their sensitivities to externally applied TEA, 4-AP, K^+ , and Cd^{2+} . Sensitivity to external Cd^{2+} indicated that approximately one-fifth of $I_{K(DR)}$ was composed of $I_{K(Ca)}$. These findings show that cultured SVZa cells have electrical properties typical of differentiating neurons.

TTX-sensitive sodium currents have also been described in subventricular zone progenitors isolated from P0–P3 rats that had been grown first as spheres of dividing cells in the presence of epidermal growth factor and then later allowed to differentiate on a polylysine/laminin substrate (Feldman et al. 1996). Interestingly, the sodium current in differentiated cells had activation kinetics similar to the neuronal type of sodium current and steady-state inactivation that resembled glial sodium current. However, undifferentiated progenitors acutely isolated from the spheres did not express sodium or potassium currents. In comparison, we observed that most (88%) precursor cells isolated from neonatal forebrain SVZa and cultured had detectable TTX-sensitive sodium currents and that all cells had potassium currents. Because we have not yet studied sodium currents in isolation, comparisons cannot be made between the sodium currents observed here and those expressed in progenitors plated from spheres.

It is difficult to relate the characteristics of the whole cell K currents that we observed to particular types of K channel α subunits. However, some α subunits can be eliminated from consideration. For example, the A-type K channels that

are blocked by TEA (Kv3.3 and 3.4) or by low external K (Kv1.4) were not present in our cells. The remaining three types of A-type K channels are Kv4.1, 4.2, and 4.3. It is possible that the Kv4.1 subunit (which is weakly expressed in olfactory bulb granule neurons) and Kv4.2 and Kv4.3 subunits (which are abundantly expressed in both olfactory bulb granule and periglomerular neurons) contribute to the A-type channel measured here. The IC_{50} for TEA on $I_{K(DR)}$ was 4.1 mM. The voltage-dependent and calcium-activated K channels with TEA sensitivity around this value include Kv1.6, 2.1, and 2.2 (Frech et al. 1989; Hwang et al. 1992; Swanson et al. 1990). However, because α subunits within a subfamily and sometimes between subfamilies can form hybrid channels, the sensitivity to TEA may reflect the most sensitive type or a combination of both sensitivities (Shahidullah et al. 1995). Thus without more evidence from antibody labeling or from subunit specific mRNA, it is not possible to identify by their TEA sensitivity which α subunits are present in the K channels.

The $I_{K(A)}$ in SVZa cells was half-inactivated at -90 mV, a value that was also observed in differentiating cerebellar granule neurons (Gorter et al. 1995). In mature granule neurons, $I_{K(A)}$ exhibits steady-state half inactivation at about -79 mV (Bardoni and Belluzzi 1993; Gorter et al. 1995). A similar change in steady-state inactivation may occur in SVZa precursor cells cultured for >1 day or in precursor cells that have migrated to the olfactory bulb. In general, the activation and inactivation kinetics of $I_{K(A)}$ were slower than those measured in mature cerebellar granule neurons (Bardoni and Belluzzi 1993; Gorter et al. 1995). These differences probably reflect the maturation state of the granule neurons because similar slow kinetics are observed in granule neurons in culture for 1 day (R. R. Stewart, P. K. Liesi, and J. M. Wright, unpublished results). Other factors that can influence the characteristics of $I_{K(A)}$ include β subunits, which have been shown to confer rapid inactivation on members of the Kv1 subfamily of K channels (Rettig et al. 1994), and γ subunits, which produce kinetics resembling $I_{K(A)}$ in mature neurons (Chabala et al. 1993; Jegla and Salkoff 1997; Serôdio et al. 1994). Whether SVZa precursor cells have β or γ subunits has not yet been determined.

In summary, after 1 day in culture, SVZa precursor cells have detectable I_{Na} , $I_{K(A)}$, and $I_{K(DR)}$ (of which a portion is calcium-activated), but are unable to generate overshooting action potentials. $I_{K(DR)}$ was blocked by TEA, inactivated slowly compared with $I_{K(A)}$, and was half-inactivated at -50 mV. The activation and inactivation kinetics and sensitivities to 4-AP and TEA of $I_{K(A)}$ resembled those of immature cerebellar granule neurons in that $I_{K(A)}$ was relatively insensitive to TEA and 4-AP and was also half inactivated at -90 mV. Although the SVZa-derived cells have not lost the capacity for division, the immature granule cells have, demonstrating that SVZa-derived cells have some properties of undifferentiated cells and some properties of differentiating cells.

We thank Dr. F. Jaramillo for allowing us to make the initial recordings in his laboratory at Emory University, Dr. W. B. Adams for critical reading of the manuscript, and Dr. A. Frankfurter for a gift of the antibody TuJ1.

This work was funded by the intramural program at the National Institute on Alcohol Abuse and Alcoholism (LMCN-SP-01) and a grant from the

National Institute of Deafness and Other Communications Disorders to M. B. Luskin.

Address for reprint requests: R. R. Stewart, Laboratory of Molecular and Cellular Neurobiology, National Institute on Alcohol Abuse and Alcoholism, Park Bldg., Rm. 118, 12501 Washington Ave., Rockville, MD 20852-1823.

Received 3 April 1998; accepted in final form 25 September 1998.

REFERENCES

- BALDWIN, T. J., TSAUR, M. L., LOPEZ, G. A., JAN, Y. N., AND JAN, L. Y. Characterization of a mammalian cDNA for an inactivating voltage-sensitive K⁺ channel. *Neuron* 7: 471–483, 1991.
- BARDONI, R. AND BELLUZZI, O. Kinetic study and numerical reconstruction of A-type current in granule cells of rat cerebellar slices. *J. Neurophysiol.* 69: 2222–2231, 1993.
- BARDONI, R., PUOPOLO, M., MAGHERINI, P. C., AND BELLUZZI, O. Potassium currents in periglomerular cells of frog olfactory bulb in vitro. *Neurosci. Lett.* 210: 95–98, 1996.
- CHABALA, L. D., BAKRY, N., AND COVARRUBIAS, M. Low molecular weight poly(A)⁺ mRNA species encode factors that modulate gating of a non-Shaker A-type K⁺ channel. *J. Gen. Physiol.* 102: 713–728, 1993.
- CULL-CANDY, S. G., MARSHALL, C. G., AND OGDEN, D. Voltage-activated membrane currents in rat cerebellar granule neurons. *J. Physiol. (Lond.)* 414: 179–199, 1989.
- DOLLY, J. O. AND PARCEI, D. N. Molecular properties of voltage-gated K⁺ channels. *J. Bioenerg. Biomembr.* 28: 231–253, 1996.
- FAGNI, L., BOSSU, J. L., AND BOCKAERT, J. Activation of a large-conductance Ca²⁺-dependent K⁺ channel by stimulation of glutamate phosphoinositide-coupled receptors in cultured cerebellar granule cells. *Eur. J. Neurosci.* 3: 778–789, 1991.
- FELDMAN, D. H., THINSCHMIDT, J. S., PEEL, A. L., PAPKE, R. L., AND REIER, P. J. Differentiation of ionic currents in CNS progenitor cells: dependence upon substrate attachment and epidermal growth factor. *Exp. Neurol.* 140: 206–217, 1996.
- FRECH, G. C., VANDONGEN, A. M., AND SCHUSTER, G. A novel potassium channel with delayed rectifier properties isolated from rat brain by expression cloning. *Nature* 340: 642–645, 1989.
- GORTER, J. A., ARONICA, E., HACK, N., BALÁZS, R., AND WADMAN, W. J. Development of voltage-activated potassium currents in cultured cerebellar granule neurons under different growth conditions. *J. Neurophysiol.* 74: 298–306, 1995.
- GRISSMER, S., NGUYEN, A. N., AIYAR, J., HANSON, D. C., MATHER, R. J., GUTMAN, G. A., KARMILOWICZ, M. J., AUPERIN, D. D., AND CHANDY, K. G. Pharmacological characterization of five cloned voltage-gated K⁺ channels, types Kv1.1, 1.2, 1.3, 1.5, and 3.1, stably expressed in mammalian cell lines. *Mol. Pharmacol.* 45: 1227–1234, 1994.
- HAMILL, O. P., MARTY, A., NEHER, E., SAKMANN, B., AND SIGWORTH, F. J. Improved patch-clamp techniques for high-resolution current recording from cells and cell-free membrane patches. *Pflügers Arch.* 391: 85–100, 1981.
- HOCKBERGER, P. E., TSENG, H.-Y., AND CONNOR, J. A. Immunocytochemical and electrophysiological differentiation of rat cerebellar granule cells in explant cultures. *J. Neurosci.* 7: 1370–1383, 1987.
- HODGKIN, A. L. AND HUXLEY, A. F. A quantitative description of membrane current and its application to conduction and excitation in nerve. *J. Physiol. (Lond.)* 117: 500–544, 1952.
- HU, H., TOMASIEWICZ, H., MAGNUSON, T., AND RUTISHAUSER, U. The role of polysialic acid in migration of olfactory bulb interneuron precursors in the subventricular zone. *Neuron* 16: 735–743, 1996.
- HWANG, P. M., GLATT, C. E., BRETT, D. S., YELLEN, G., AND SNYDER, S. H. A novel K⁺ channel with unique localizations in mammalian brain: molecular cloning and characterization. *Neuron* 8: 473–481, 1992.
- JANKOVSKI, A. AND SOTELO, C. Subventricular zone olfactory bulb migratory pathway in the adult mouse: cellular composition and specificity as determined by heterochronic and heterotopic transplantation. *J. Comp. Neurol.* 371: 376–396, 1996.
- JEGLA, T. AND SALKOFF, L. A novel subunit for Shal K⁺ channels radically alters activation and inactivation. *J. Neurosci.* 1: 32–44, 1997.
- LEE, M. K., TUTTLE, J. B., REBHUN, L. L., CLEVELAND, D. W., AND FRANKFURTER, A. The expression and posttranslational modification of a neuron-specific beta-tubulin isotype during chick embryogenesis. *Cell Motil. Cytoskel.* 17: 118–132, 1990.

- LUSKIN, M. B. Restricted proliferation and migration of postnatally generated neurons derived from the forebrain subventricular zone. *Neuron* 11: 173-189, 1993.
- LUSKIN, M. B. AND BOONE, M. S. Rate and pattern of migration of lineally-related olfactory bulb interneurons generated postnatally in the subventricular zone of the rat. *Chem. Senses* 6: 695-714, 1994.
- LUSKIN, M. B., ZIGOVA, T., SOTERES, B. J., AND STEWART, R. R. Neuronal progenitor cells derived from the anterior subventricular zone of the neonatal rat forebrain continue to proliferate in vitro and express a neuronal phenotype. *Mol. Cell. Neurosci.* 8: 351-366, 1997.
- MAGRASSI, L. AND GRAZIADEI, P. P. Cell death in the olfactory epithelium. *Anat. Embryol.* 192: 77-87, 1995.
- MENEZES, J.R.L. AND LUSKIN, M. B. Expression of neuron-specific tubulin defines a novel population in the proliferative layers of the developing telencephalon. *J. Neurosci.* 14: 5399-5416, 1994.
- ONO, K., TOMASIEWICZ, H., MAGNUSON, T., AND RUTISHAUSER, U. N-CAM mutation inhibits tangential neuronal migration and is phenocopied by enzymatic removal of polysialic acid. *Neuron* 13: 595-609, 1994.
- PAK, M. D., BAKER, K., COVARRUBIAS, M., BUTLER, A., RATCLIFFE, A., AND SALKOFF, L. mShal, a subfamily of A-type K⁺ channel cloned from mammalian brain. *Proc. Natl. Acad. Sci. USA* 88: 4386-4390, 1991.
- PARDO, L. A., HEINEMANN, S. H., TERLAU, H., LUDEWIG, U., LORRA, C., PONGS, O., AND STÜHMER, W. Extracellular K⁺ specifically modulates a rat brain K⁺ channel. *Proc. Natl. Acad. Sci. USA* 89: 2466-2470, 1992.
- RETTIG, J., HEINEMANN, S. H., WUNDER, F., LORRA, C., PARCEJ, D. N., DOLLY, J. O., AND PONGS, O. Inactivation properties of voltage-gated K⁺ channels altered by presence of β -subunit. *Nature* 369: 289-294, 1994.
- RUDY, B. Diversity and ubiquity of K channels. *Neuroscience* 25: 729-749, 1988.
- SCHRÖTER, K.-H., RUPPERSBERG, J. P., WUNDER, F., RETTIG, J., STOCKER, M., AND PONGS, O. Cloning and functional expression of a TEA-sensitive A-type potassium channel from rat brain. *Fed. Eur. Biochem. Soc.* 278: 211-216, 1991.
- SERÓDIO, P., DE MIERA, E.V.S., AND RUDY, B. Cloning of a novel component of A-type K⁺ channels operating at subthreshold potentials with unique expression in heart and brain. *J. Neurophysiol.* 75: 2174-2178, 1996.
- SERÓDIO, P., KENTROS, C., AND RUDY, B. Identification of molecular components of A-type channels activating at subthreshold potentials. *J. Neurophysiol.* 4: 1516-1529, 1994.
- SERÓDIO, P. AND RUDY, B. Differential expression of Kv4 K⁺ channel subunits mediating subthreshold transient K⁺ (A-type) currents in rat brain. *J. Neurophysiol.* 79: 1081-1091, 1998.
- SHAHIDULLAH, M., HOSHI, N., YOKOYAMA, S., AND HIGASHIDA, H. Microheterogeneity in heteromultimeric assemblies formed by *Shaker* (Kv1) and *Shaw* (Kv3) subfamilies of voltage-gated K⁺ channels. *Proc. R. Soc. Lond. B Biol. Sci.* 261: 309-317, 1995.
- STEWART, R. R., BOSSU, J. L., MUZET, M., DUPONT, J.-L., AND FELTZ, A. Voltage-activated ionic currents in differentiating rat cerebellar granule neurons cultured from the external germinal layer. *J. Neurobiol.* 28: 419-432, 1995.
- STÜHMER, W., RUPPERSBERG, J. P., SCHRÖTER, K. H., SAKMANN, B., STOCKER, M., GIESE, K. P., PERSCHKE, A., BAUMANN, A., AND PONGS, O. Molecular basis of functional diversity of voltage-gated potassium channels in mammalian brain. *EMBO J.* 8: 3235-3244, 1989.
- SWANSON, R., MARSHALL, J., SMITH, J. S., WILLIAMS, J. B., BOYLE, M. B., FOLANDER, K., LUNEAU, C. J., ANTANAVAGE, J., OLIVA, C., BUHROW, S. A., BENNETT, C., STEIN, R. B., AND KACZMAREK, L. K. Cloning and expression of cDNA and genomic clones encoding three delayed rectifier potassium channels in rat brain. *Neuron* 4: 929-939, 1990.
- TOMASIEWICZ, H., ONO, K., YEE, D., THOMPSON, C., GORIDIS, C., RUTISHAUSER, U., AND MAGNUSON, T. Genetic deletion of a neural cell adhesion molecule variant (N-CAM-180) produces distinct defects in the central nervous system. *Neuron* 11: 1163-1174, 1993.
- VEGA-SAENZ DE MIERA, E., MORENO, H., FRUHLING, D., KENTROS, C., AND RUDY, B. Cloning of ShIII (Shaw-like) cDNAs encoding a novel high-voltage-activating, TEA-sensitive, type-A K⁺ channel. *Proc. R. Soc. Lond. B Biol. Sci.* 248: 9-18, 1992.
- ZIGOVA, T., BETARBET, R., SOTERES, B. J., BROCK, S., BAKAY, R.A.E., AND LUSKIN, M. B. A comparison of the patterns of migration and the destinations of homotopically transplanted neonatal subventricular zone cells and heterotopically transplanted telencephalic ventricular zone cells. *Dev. Biol.* 173: 459-474, 1996.